Modelling Microstructural Evolution in Cast Alloys

Prof. Rachel C. Thomson

Institute of Polymer Technology and Materials Engineering,
Loughborough University, UK

Abstract

The most appropriate choice of metal alloy is vital for the successful implementation of engineering components. In many cases, the properties will change as a result both of the initial processing and the subsequent service life of a component, and therefore it is essential to understand how and why such changes occur. In recent years there have been significant developments in the ability to predict both the initial structure of an alloy and its subsequent evolution. This paper highlights the importance of these modelling approaches by considering a number of different engineering components. For example, in the automotive industry, the models have been used to predict and improve the properties of aluminium alloys for car pistons and cast irons for camshafts. The advantage of modelling microstructural evolution is to potentially reduce alloy development lead times by predicting the microstructure and properties of a particular alloy, thereby minimising the number of necessary experimental trials. The ultimate aim is, however, to predict not only the initial microstructure, but also the mechanical properties, and any changes during the service life of a component. This is a significant challenge, particularly for properties such as fatigue behaviour, which are a complex function of a number of variables. In addition to recent advances in modelling capability, there have also been developments in advanced characterisation techniques. These include, for example, electron back scatter diffraction and depth sensing indentation, which allow a more rapid determination of microstructural features, and provide a route to linking microstructure and mechanical property predictions to provide a total product design concept.

Key words

Modelling, Microstructural Evolution, Austempered Ductile Iron, Al-Si

Introduction

The ultimate aim of computational materials science is to model the complete through-process behaviour of materials from primary processing all the way to final component properties and their subsequent service behaviour. This is particularly true for metallic solidification processing in which there are many different phenomena which need to be considered: fluid flow and heat transfer, both liquid/solid and solid state phase transformations, defect evolution, grain structure evolution and recrystallisation, recalesence from latent heat evolution, and the presence of residual stresses. Such models are needed because the properties of industrial components are essentially determined by their microstructure, which results primarily from interactions during and subsequent to solidification at the micro-, meso- and macro-scale. This is a significant challenge, as discussed by Voller [1], and requires the development of new modelling methodologies which can capture the behaviour across micro to macro length and timescales. Nevertheless, there are a number of extremely useful and successful modelling approaches which are used in the production of cast alloys. These have been comprehensively reviewed by Rappaz [2] and Stefanescu [3], and tracked in the proeedings of the MCWASP conference series [4].

There are now commercial software tools which can cope with most of the continuum phenomena involved in solidification processing (e.g. MAGMA, PROCAST, FLOW3D). They take into account heat transfer, fluid flow and can simulate the filling of the mould cavity by molten metal and its subsequent solidification, usually based on finite difference or finite element methodologies. Microstructural features form and evolve during each of the processing steps as a function of the macroscopic heat, mass and momentum transfer. The prediction of grain size has been modelled by deterministic, cellular automata [e.g. 5] and phase field methodologies. Cellular automata methods include effects such as impingement, and can predict not only the average grain size, but also distributions of grain sizes and morphologies. Phase field methods allow the incorporation of thermodynamic data and parameters such as interfacial energies, and are potentially very powerful, although are computationally expensive.

Fine scale features within the microstructure, such as the formation of multiple phases within a particular alloy system have received less attention, but are extremely important in the determination of the properties of the alloy. Thermodynamic calculations can be performed by commercial packages, for example, Thermocalc and MTDATA, which will predict the phases likely to be present in a given alloy. These packages rely upon critically assessed thermodynamic data and use an exceptionally reliable Gibbs free energy minimisation algorithm to predict the phases present at thermodynamic equilibrium. In recent years the quality of thermodynamic databases has improved greatly and there are now a number of databases available which contain data for the large number of elements and phases which are present in cast alloys, including Al, Ni and Fe based alloys of importance in the foundry industry. Predictions generally relate to

thermodynamic equilibrium as a function of composition, temperature and pressure, however, it is possible to apply calculations to non-equilibrium phenomena. These include the prediction of precipitation sequences in alloys by making a prediction, then preventing the phase predicted to be stable from being present, and running the calculation again to establish the next most stable phase, or by using a Scheil approach to model segregation during solidification of an alloy.

This paper will demonstrate the application of thermodynamic and kinetic models to the prediction of microstructural evolution in cast alloys using two specific examples. In the first, austempered ductile iron, thermodynamic calculations are used to predict the segregation behaviour in a casting, and combined with a kinetic model for the subsequent solid state phase transformation of the matrix. In the second, multicomponent Al-Si casting alloys, a phase field methodology coupled to thermodynamic calculations is described which can allow for the prediction of the morphology of phases in addition to their formation temperatures and overall mass fraction. There is also brief discussion of advanced characterisation techniques for microstructural assessment and strategies which can be used to determine structure/property relationships.

Microstructural Evolution in Austempered Ductile Cast Iron

Austempered ductile cast iron (ADI) results from the heat treatment of ductile cast iron. After casting, a component undergoes a two step heat treatment which involves an austenitising step, typically in the temperature range 850-1050^{o}C, followed by an austempering step in the temperature range 200-400^{o}C, and is subsequently cooled to room temperature. This results in a microstructure comprising spheroidal graphite, in a matrix of bainitic ferrite together with some retained austenite (often referred to as ausferrite in cast iron). The solid state phase transformations are greatly affected by the composition of the alloy, and in particular the carbon concentration of the austenite prior to the bainite transformation, which in turn is a result of the austenitising temperature and time. ADI originates from a cast microstructure, and therefore there is also chemical segregation present in the alloy as a result of the initial solidification process. In order to model the microstructural evolution, and therefore mechanical properties, it is therefore necessary to consider each step within the process. First, the as-solidified microstructure must be predicted, with respect to both graphite distribution and chemical segregation. The equilibrium between austenite and graphite at the austenitising temperature can then be considered to determine the carbon concentration in the matrix prior to transformation to bainite, and subsequently the kinetics of the bainite transformation itself must be predicted during the austempering process. A final step is to predict whether any martensite will also form within the microstructure on final cooling to room temperature.

Prediction of the As-Cast Microstructure

The prediction of the initial graphite distribution during the solidification of cast iron is difficult, and is a complex function of a number of factors. Nevertheless, it is possible to use thermodynamic calculations [6] to predict the likely chemical segregation using a Scheil methodology in which the solute redistribution is modelled [7]. The Scheil approach assumes no diffusion in the solid and unlimited diffusion in the liquid, and has been shown to agree reasonably with experimental results if the very last solid is ignored [8]. Nastac and Stefanescu developed a model that accounts for diffusion in both the liquid and solid states [9]. Liu and Elliot have also produced a numerical microsegregation model taking into account diffusion in both the solid and liquid, interface movement, non linear growth rates and total solute conservation [10]. Both methods have been shown to be in good agreement with measured segregation profiles.

The starting point for calculation of the likely segregation during casting is the composition of the alloy, which is input into a series of thermodynamic equilibrium calculations performed over a suitable temperature range in order to find the liquidus temperature. Once the liquidus temperature has been found, the system temperature can be set to a small amount below it (e.g. 0.5^{o}C) and a further equilibrium calculation performed. The mass and chemical composition of any solids (austenite and graphite) that are predicted to form in this step are recorded and removed from the system so only liquid remains. The temperature is then reduced by a further 0.5^{o}C, and the process repeated until less than 0.005% of the original liquid mass remains in the system, when solidification is assumed to be complete. It is necessary to 'relocate' the graphite because an artefact of applying Scheil solidification to this system is that graphite forms at each step, the amount of which depends on the solubility of carbon in austenite. The sum of the amount of graphite in the steps is equivalent to the whole of the graphite nodule(s), but must be relocated in accordance with the observed microstructure, therefore the graphite calculated to form in each of the steps was assumed to form in one location only, equivalent to one nodule, and was adjacent to the first solid to form. This process is illustrated schematically in Figure 1.

The first and last steps are assumed to be next to the nodule and halfway between two nodules respectively (i.e. they represent the first and last liquid to solidify). Since the chemical composition of the austenite in each step is recorded, a chemical composition profile can be produced as a function of distance from the nodule. The chemical composition profile can then be divided into an arbitrary number of regions of equal mass starting with material close to the nodule and working progressively outwards. Hence regions of differing composition are obtained which simulate the composition profile found between a nodule and a cell boundary.

It is possible to compare the predictions of the Scheil approach with experimental measurements of the chemical segregation within a casting,

typically carried out using energy dispersive X-ray analysis in a scanning electron microscope (SEM). An illustration is given in Figure 2, in which the predictions of the model are compared with experimental measurements for a particular ductile cast iron. Over 1000 composition measurements are included in the graph, which have undergone a statistical analysis following [11], and represent the overall segregation pattern. It can be seen that there is good agreement between the two, with Cu and Si being predicted to segregate to the graphite nodule, and Mn being found in higher concentrations in the last liquid to solidify, half way between graphite nodules. It is acknowledged that the nodule count will have an influence on the segregation behaviour during solidification [12]; if there is a relatively low nodule count, as in the example shown in Figure 2, then this methodology is appropriate, however, for alloys with a higher nodule count, their segregation profile might be expected to be less severe which may result in a reduced accuracy to the model. Additional modifications are necessary to take into account fully the behaviour of the nodules within the ductile iron casting, nevertheless this approach allows subsequent modelling of the austenitising and austempering process across an inhomogeneous material.

Austenitisation

The composition profile of the substitutional elements is assumed not to change during the subsequent austenitisation and austempering heat treatments. In order to model the austenitisation step, each of the regions can then be assigned the alloy carbon content, assuming carbon diffusion is extremely rapid, and an equilibrium calculation performed for each region to determine the carbon content of the austenite and the mass of graphite stable at the austenitising temperature. This simple calculation can also be very important for determining which elements within the specification are most important to control in respect of the subsequent solid state transformations. Figure 3 illustrates a sensitivity study in which the concentration of each of the elements was varied in turn in respect to the amount in the base alloy, and clearly shows that it is primarily the Si, and to a lesser extent the Cu and Mn, concentrations which affect the carbon concentration in austenite the most.

Austempering

The austempering heat treatment is also very important in determining the exact microstructure produced and can itself be considered to occur in a series of stages. In the first stage of the austempering process, the metastable austenite will transform into a mixture of bainitic ferrite and high carbon austenite. The exact temperature employed in the austempering process will affect the structure of the bainitic ferrite – at the higher austempering temperatures within the range, the bainite will be carbide free (c.f. upper bainite in steels) whereas at the lower temperatures the bainite transformation may be accompanied by carbide precipitation (c.f. lower bainite in steels), resulting in a mixture of bainitic ferrite, carbide and high carbon austenite. The high carbon austenite will

eventually decompose into a mixture of thermodynamically more stable ferrite and carbide on prolonged heat treatment; this is termed the Stage II reaction. Hence, there is a well-defined processing window during which time a relatively stable structure of bainitic ferrite and high carbon austenite, often termed 'ausferrite', exists between the Stage I and Stage II reactions.

The most significant microstructural changes occur during Stage I of the austempering process, and therefore this part of the reaction has been the primary focus of models to date. It has also been assumed that the high Si content present in ADI will largely prevent the formation of carbide during the Stage I reaction at the lower austempering temperatures, and therefore any carbide formation accompanying the bainite reaction has not been taken into consideration. Predictions are therefore realistic for commercial alloys which are heat treated within a processing window before significant onset of the Stage II reaction.

Supersaturated austenite transforms to supersaturated bainitic ferrite via a displacive mechanism, and following the transformation, carbon diffuses from the bainitic ferrite to the remaining austenite. This leads to an increase in the austenite carbon content and hence to a reduction in the Gibbs energy difference between the two phases, the driving force for the reaction. The diffusionless transformation ceases when the driving force reaches zero, leading to the 'incomplete reaction phenomenon'. The maximum carbon content at which the transformation can occur increases with decreasing austempering temperature. Calculation of this carbon content, x_{T*}, can be carried out by calculating the free energies of austenite and ferrite at the appropriate temperature using thermodynamic data. The maximum volume fraction of bainitic ferrite, V_b, can then be calculated for the alloy composition of interest using the lever rule:

$$V_b = \frac{x_{T*} - x_\gamma}{x_{T*} - x_\alpha} \quad (1)$$

The matrix carbon content, x_γ, is taken as the value determined from the calculation of the austenite/graphite equilibria at the austenitising temperature, and the carbon content of the (saturated) ferrite, x_α, is calculated at the austempering temperature using a polynomial expression derived from empirical data [13]. In addition to the calculation of the overall amount of bainite formed, it is also possible to calculate its rate of formation by modifying a model developed for low alloy steels [14, 15] and adapted for ADI [16]. A prediction of the transformation kinetics is useful for the determination of production heat treatment times, allowing estimation of the processing window for particular time / temperature / composition combinations. Figure 4 gives an example prediction for the major phases in a particular ADI alloy heat treated under different austenitising and austempering conditions, and shows that the austempering temperature has a greater effect on the proportions of phases within the microstructure than the austenitising temperature, as

expected. This combined thermodynamic and kinetic modelling approach, albeit with some simplifying assumptions, allows prediction of microstructure as a result of both solidification and heat treatment in these complex alloys and can be used to reduce alloy development time.

Prediction of Structure/Property Relationships

The ultimate goal of microstructure modelling methodologies is to be able to relate the predicted microstructure to mechanical properties, hence allowing alloy design by computer to produce components with the desired performance.

Properties of particular interest for ADI components include tensile strength, hardness, fatigue [17], ductility, toughness and wear resistance. The prediction of complex mechanical properties, such as fatigue behaviour and toughness is difficult from first principles, and may be approached using methodologies such as neural networks [e.g. 18]. However, 'simpler' properties such as yield strength, can be approached using a law of mixtures approach similar to that for composite materials, i.e. that each phase contributes proportionally to the overall strength weighted by mass fraction. This approach relies on models being available for the strength of each of the individual components within the microstructure [16]. Figure 5 demonstrates the results of such a model, and shows a comparison of the predicted austenite volume fractions and experimental values reported in the literature for a variety of ductile iron compositions, austenitising temperatures and times. There is some degree of overestimation of the yield strength for the lower end of the strength range, probably due to small errors in the prediction of the volume fraction of bainitic ferrite and some underestimation at the higher strength range, possibly due to the neglect of carbide formation within the microstructure. Nevertheless, it can be seen that this simple approach is able to predict the yield strength of different ADI alloys relatively well.

Microstructural Evolution in Al-Si Alloys

Multicomponent Al-Si based casting alloys are used for a variety of engineering applications, including for example, piston alloys. Properties include good castability, high strength, light weight, good wear resistance and low thermal expansion. In order for such alloys to continue operation to increasingly high temperatures, alloy element modifications are continually being made to further enhance the properties. Improved mechanical and physical properties are strongly dependent upon the morphologies, type and distribution of the second phases, which are in turn a function of alloy composition and cooling rate. The presence of additional elements in the Al-Si alloy system allows many complex intermetallic phases to form, which make characterisation non-trivial due to the fact that some of the phases have either similar crystal structures or only subtle changes in their chemistries. These include, for example, $CuAl_2$, Al_3Ni_2, Al_7Cu_4Ni, Al_9FeNi and $Al_5Cu_2Mg_8Si_6$ phases, all of which may have some solubility for additional elements.

Thermodynamic Prediction of the Phases Present

It is possible to carry out simple thermodynamic calculations for multicomponent Al-Si alloys to predict the phases which are likely to be present as a function of variation in chemical composition. Thermodynamic databases are available which contain appropriate parameters for these complex multicomponent alloys [e.g. 19] and can take into account most, if not all, of the elements present. It is recognised that cast microstructures are not necessarily in their equilibrium state, nevertheless such calculations provide a useful insight into phase stability. Figure 6 presents the results of such thermodynamic equilibrium calculations and plots the mass fraction of the minor phases predicted to be present under both equilibrium and Scheil cooling conditions. The majority of the microstructure is predicted to comprise an Al matrix together with approximately 10% Si particles (not shown), with a number of intermetallic phases being predicted to be present in relatively small amounts. It is interesting to note that in general the predictions agree very well with experimental observations, with the two intermetallics (αAlFeSi and Al_9FeNi) predicted to be present in the largest quantities being those observed in the highest quantities experimentally. The Scheil calculations provide an insight into the phases which are likely to be found as a result of chemical segregation which occurs on solidification, and indeed one of the phases (βAlFeSi), which was only observed experimentally in small quantities within particular regions of the microstructure, was only predicted to occur using a Scheil methodology. It has been demonstrated, therefore, that thermodynamic calculations are very useful as a tool to guide alloy development. However, their significant limitation is that they can provide no information about the morphology of the phases present, which may have a critical influence on the mechanical behaviour.

Prediction of the Morphology of the Phases: Phase Field Modelling

One possible route to the prediction of not only the amount, but also the morphology, of phases present in a particular alloy system is the use of phase field modelling techniques. Classical solidification models are often termed ‘sharp interface’ models in which the solid-liquid boundary is described as a two dimensional surface with no internal structure or width. It is then necessary to track the position of the boundary during the entire solidification process in order to apply the relevant equations of motion, and is relatively complex to implement numerically. The phase field method instead relies on an order parameter to describe the physical state of the system (e.g. liquid or solid), and therefore the solid-liquid interface has a finite thickness. Solidification can then be described in terms of the evolution of this parameter, hence removing the need for interface tracking. The phase field method can incorporate the nucleation and growth of matrix and second phase particles, and has the potential to be directly linked to thermodynamic data and phase diagram information, and therefore to the modelling of solidification in complex multi-element, multi-phase systems.

There have been a number of phase-field models published dealing with the solidification. The earliest phase-field models for the solidification of pure substances were developed in the mid 1980s by a number of authors [20-22]. Wheeler et al. developed the first phase-field model for binary alloy solidification [23], and the model has been successfully applied to a number of cases [24, 25]. Steinbach et al. introduced a binary-multiphase field model [26], which has been used to successfully model the solidification of eutectic, peritectic and monotectic alloys [27, 28]. Ode et al. developed a phase-field model for ternary alloys [29]. Miyazaki [30] and Cha et al. [31] have developed phase-field models that are suitable for the study of multicomponent alloys, and recently a phase-field model appropriate for the simulation of a 'real' alloy that contains multiple components and multiple solid phases has been reported [32].

An example of a phase field simulation carried out for a binary Al-Si alloy is presented in Figure 7, in which the development of the eutectic structure can be seen to compare favourably with experimental observations. A more complex phase field simulation is illustrated in Figure 8, for an Al-Si-Cu-Fe alloy. The matrix, Al, forms the majority phase, with Si present at ~10% and additionally two intermetallics are predicted to be stable in this system; the δAlFeSi can form from the liquid, with $CuAl_2$ being predicted to be stable at lower temperatures below 500^{o}C. A number of parameters are required for the phase field simulations, which include interfacial energies, chemical diffusion coefficients, together with a parameter which represents the likely anisotropy of each phase. It is not always possible to find experimental data for each of the parameters needed, and therefore sensitivity studies may be necessary to ensure an appropriate simulation can be carried out for different alloy systems. However, the potential of the phase field method to simulate the morphologies of phases and their relative distributions in multicomponent, multiphase alloys is clear, and there are exciting possibilities to link this to other modelling strategies to provide a complete model of the solidification process.

Advanced Characterisation Techniques

It is essential that models of microstructural evolution are validated to ensure fitness for purpose and to ensure that they accurately represent the observed phenomena within the particular alloy. In addition to 'conventional' techniques, there are a number of characterisation techniques which have developed significantly in recent years such that they are widely available for more routine characterisation. Examples are electron back scatter diffraction (EBSD), an attachment for a scanning electron microscope, and depth sensing indentation (nanoindentation).

Electron Back Scatter Diffraction

Electron backscatter diffraction (EBSD) is used for the crystallographic analysis of fine scale regions within bulk specimens and has primarily been used as tool for mapping the crystallographic orientation of known

polycrystalline samples. More recently it has also been used, typically in conjunction with a crystallographic database, for the identification of unknown crystalline phases in bulk specimens. The specimen surface is typically highly polished, and should be strain free. Kikuchi bands are produced from the interaction of the electron beam with the sample. These bands reflect the symmetry of the crystal lattice, and the width and intensity of the bands are directly related to the interplanar spacing [33]. Figure 9 illustrates the conventional use of EBSD in the determination of grain boundaries and grain orientations for a section of a casting in which there is a columnar region at the edge of the casting, and an equiaxed region towards the centre, together with a very fine 'transition' region between the two. This technique is very useful for quantitative studies of grain refinement in cast alloys.

It is also possible to simultaneously collect chemical data by conventional energy dispersive X-ray (EDX) analysis in order to better discriminate between phases using both chemical and crystallographic data. Figure 10 illustrates the benefit of this technique for the rapid identification of phases in a complex multicomponent Al-Si alloys. Figure 10a shows an SEM image of what is apparently a single intermetallic particle, however, the image quality map, a measure of the quality of the electron diffraction patterns, indicates differential contrast across the particle indicative of the presence of more than one phase. The EDX maps in Figures 10b and c for Cu and Ni respectively clearly show a difference in composition across the particle, matched by a difference in orientation in Figure 10e. The phase map in Figure 10f obtained by the combined use of EDX and EBSD to discriminate the different phases present clearly shows that in fact the particle is composed of three different phases which have formed from each other as solidification proceeds. This type of detailed analysis is important in the determination of solidification sequences and provides an insight into the complex nature of phase formation in multicomponent casting alloys.

Depth sensing indentation

Depth sensing indentation (DSI) is commonly referred to as nanoindentation since the technique usually operates in the sub-micron depth range with nanometer resolution [34]. DSI is an important technique for probing the mechanical behavior of materials, particularly hardness and modulus, at small length scales via continuously recording the force applied and the corresponding displacement during an indentation. This technique therefore offers the possibility of the measurement of local mechanical properties for particular phases within an alloy system. Figure 11 presents hardness and modulus data obtained by nanoindentation in the particle analysed in Figure 10 and clearly shows that there is a significant variation in mechanical properties across the complex particle. The Al_2Cu phase is found to be considerably softer than the Cu and Ni containing phases, with the Al_3Ni_2 phase being slightly harder than the Al_7Cu_4Ni phase. It is also possible, through the use of a hot stage, to

obtain the temperature dependence of the mechanical properties of individual phases. These differential mechanical properties may have important implications for the performance of alloys in service and therefore their assessment through the use of advanced techniques are important component parts within an overall modelling strategy.

Conclusions

In the first example of austempered ductile iron, a combination of equilibrium thermodynamics and kinetic theory has been used to successfully predict the amounts of the major phases, austenite, graphite, bainite and martensite, which occur as a function of heat treatment time and temperature. The inherent segregation present in the microstructure has also been considered using a Scheil approach, which enables predictions to be made of the microstructural constituents as a function of position relative to graphite nodules. In the second example, the potential of phase field approaches to predict not only the relative amount, but also the morphology of phases in multicomponent, multiphase systems. The potential contribution that advanced characterisation techniques can make to the validation of through process models has also been highlighted.

The modelling of microstructural evolution during solidification of cast alloys is an exciting field which has developed rapidly in recent years. The next significant challenge is the genuine two-way coupling of models across length and time scales, incorporating links between microstructural evolution and mechanical property prediction, which combined with the continuing availability of increased computer power, is likely to provide new insights into, and potential control of, solidification processing for industrial applications.

References

1. Voller V R, Micro-macro modelling of solidification processes and phenomena, MCWASP Conference Proceedings, TMS, 2001, pp 41
2. Rappaz M, International Materials Reviews, 34(3), 1989, pp 93
3. Stefanescu D M, ISIJ, 35(6), 1995, pp 637
4. MCWASP Conference Proceedings series, TMS (1980 – 2003)
5. Spittle J A and Brown S G R, Acta Met, 37, 1989, pp 1803
6. Davies R H, Dinsdale A T, Chart T G, Barry T I and Rand M, High Temperature Science, 26, 1989, pp 251
7. Scheil E, Zeitschrift Metallkunde, 34, 1942, pp 70
8. Boeri R and Weinberg F, AFS Transactions, 97, 1990, pp 179
9. Nastac L and Stefanescu D M, AFS Transactions, 101, 1993, pp 933
10. Liu J and Elliott R, Materials Science and Technology, 14, 1998, pp 1127
11. Hayrynen K L, Moore D J, Rundman K B, AFS Transactions, 96, 1988, pp 619
12. Liu J and Elliott R, International Journal of Cast Metals Research, 12, 1999, pp 75
13. Bhadeshia H K D B, Metal Science, 16, 1982, pp 167

14. Chester N and Bhadeshia H K D H, Journal de Physique, C5, 1997, pp 41
15. Bhadeshia H K D B, 'Bainite in Steels', 1992, London, Institute of Materials.
16. Thomson R C, James J S and Putman D C, Materials Science and Technology, 16, 2000, pp 1412
17. Reed P A S, Thomson R C, James J S, Putman D C, Lee K K and Gunn S R, Materials Sci. and Engineering A, 346(1-2), 2003, pp 273
18. Yescas M A, Bhadeshia H K D H, MacKay D J, Materials Science And Engineering A, 311 (1-2), 2001, pp 162
19. Saunders N, Materials Science Forum, 217, 1996 pp 667
20. Collins J B and Levine H, Phys. Rev. 31B, 1985, pp 6119
21. Langer J S, in: Grinstein G and Mazenko G (Eds.), Directions in Condensed Matter, World Scientific, Singapore, 1986, p. 164.
22. Caginalp G and Fife P, Phys. Rev. 33B, 1986, pp 7792
23. Wheeler A A, Boettinger W J and McFadden G B, Phys. Rev. 45A, 1992, pp 7424
24. Warren J A and Boettinger W J, Acta Metall. Mater., 43, 1995, pp 689
25. Murray B T, Wheeler A A and Glicksman M E, J. Crys. Growth, 154, 1995, pp 386
26. Steinbach I, Pezzolla F, Nestler B, Rezende J, Seeßelberg M and Schmiz G J, Physica, 4D, 1996, pp 135
27. Nestler B and Wheeler A A, Physica, 138D, 2000, pp 114
28. Nestler B and Wheeler A A, Comp. Phys. Com., 147, 2002, pp 230
29. Ode M, Lee J S, Kim S G, Kim W T and Suzuki T, ISIJ Inter. 9, 2000, pp 870
30. Miyazaki T, CALPHAD, 25, 2001, pp 231
31. Cha P R, Yeon D H and Yoon J K, Acta Mater., 49, 2001, pp 3295
32. Qin R S, Wallach E R and Thomson R C, Journal of Crystal Growth, 279(1-2), 2005, pp 163
33. Schwartz A J, Kumar M, Adams B L, Electron Backscatter Diffraction in Materials Science. Kluwer Acadamic/Plenum Publishers, 2000.
34. Oliver W C, Pharr G M, J. Mater. Res., 7, 1992, pp 1564
35. Putman D C and Thomson R C, International Journal of Cast Metals Research, 16(1), 2003, pp 191
36. Chen C-L and Thomson R C, Private Communication, 2006.

Acknowledgements

The author would like to thank EPSRC for financial support under GR/M38667/01 and past and present members of her research group: in particular Wendy Adams, Chun-Liang Chen, Joss James, Duncan Putman and Rongshan Qin who have all contributed to this research. Fruitful collaboration with Dr Philippa Reed and her group at Southampton University is gratefully acknowledged, together with helpful discussions and support from the MTDATA team, Thermodynamic and Process Modelling Group, NPL, UK, concerning the thermodynamic calculations.

Contact Email: R.C.Thomson@lboro.ac.uk

Figures

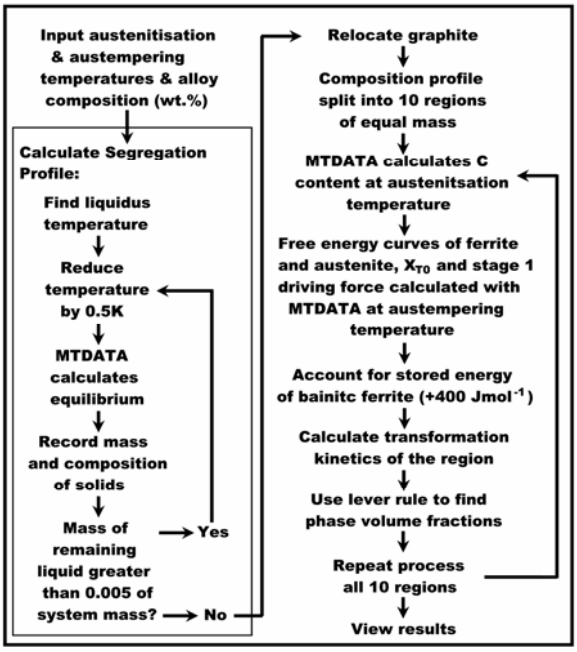

Figure 1: A schematic flow diagram of the Scheil approach to modelling solidification [35].

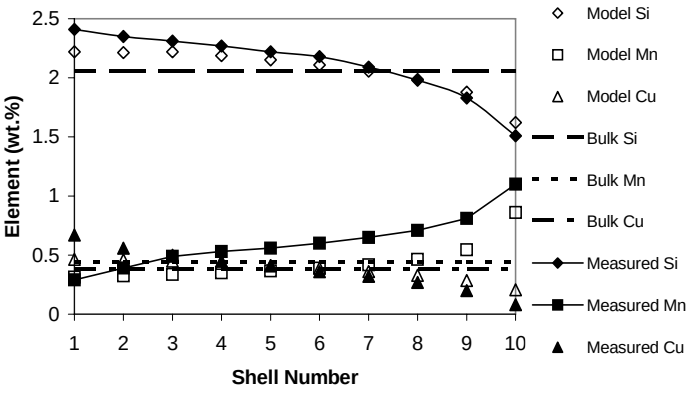

Figure 2: A comparison of segregation profiles predicted using the Scheil methodology and measured using EDX analysis in the SEM [35].

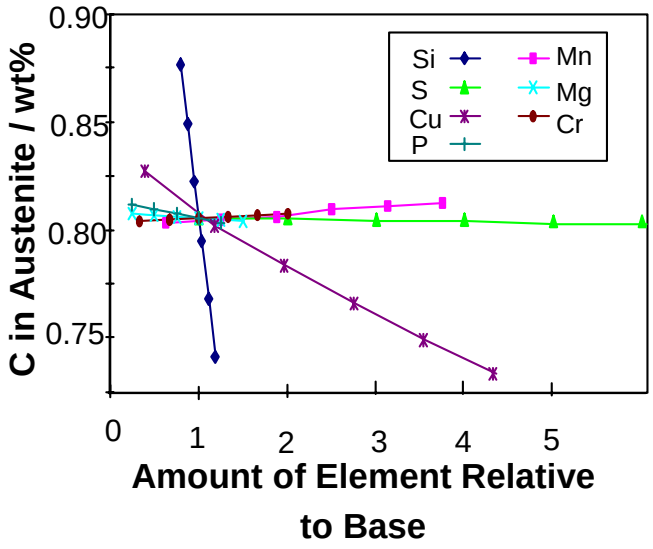

Figure 3: Prediction of the austenite carbon content as a function of alloy composition [16].

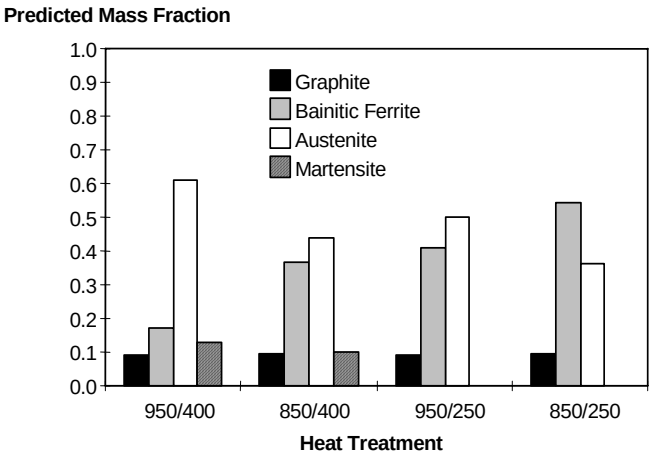

Figure 4: An example prediction for the major phases in a particular ADI alloys. Figures on the bottom axis are the austenitisation temperature and austempering temperature (°C) respectively, with both heat treatments being carried out for 60 minutes [16].

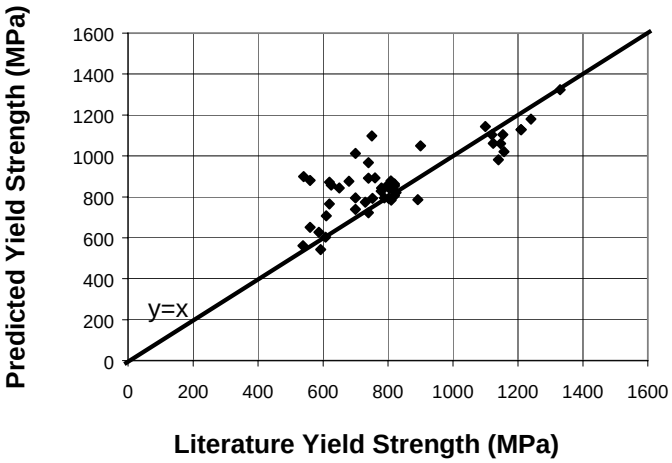

Figure 5: A comparison of the predicted yield strength and experimental values reported in the literature for a variety of austempered ductile iron compositions, austenitising and austempering temperatures and times [16].

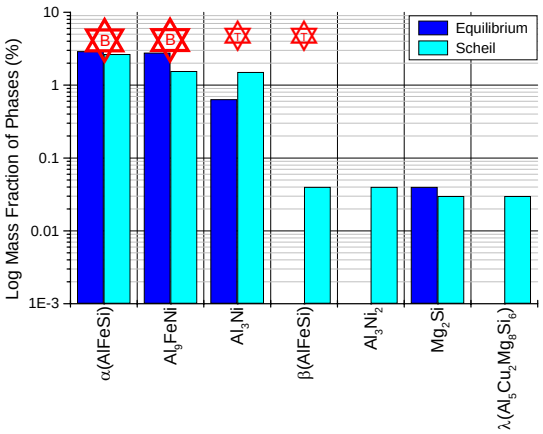

Figure 6: Phases predicted to be present under both equilibrium and Scheil cooling conditions in a multicomponent Al-Si alloys. The phases which were found to be present in the alloy using microscopy techniques in substantial amounts within the bulk of the sample are denoted by ‘B’ and those observed in trace quantities by ‘T’.

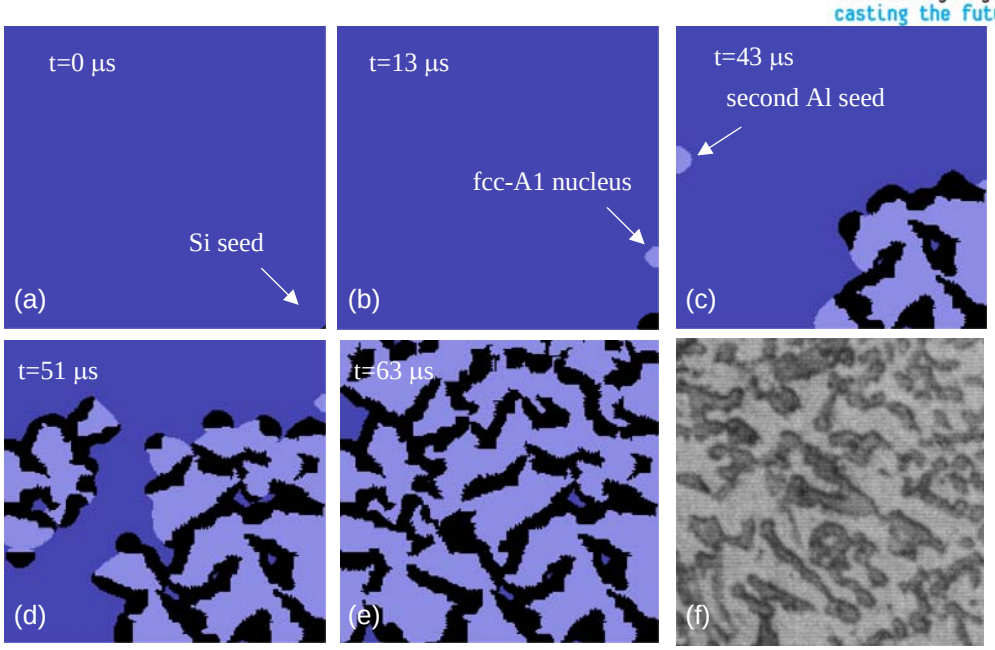

Figure 7: Phase field simulation (images a to e) of solidification in a binary Al-Si eutectic alloy, compared with an optical microscope image (f).

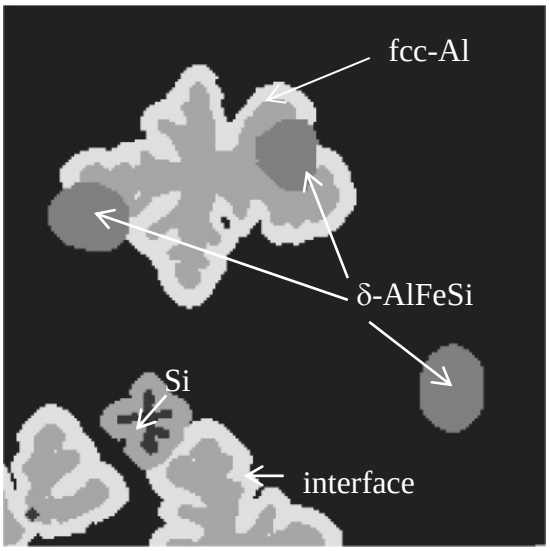

Figure 8: The distributions of phase-field order parameters at *t*=340 μs showing the morphologies of fcc-Al, Si and δ-AlFeSi particles at 830 K in the simulation of solidification in an AlSiCuFe alloy [32].

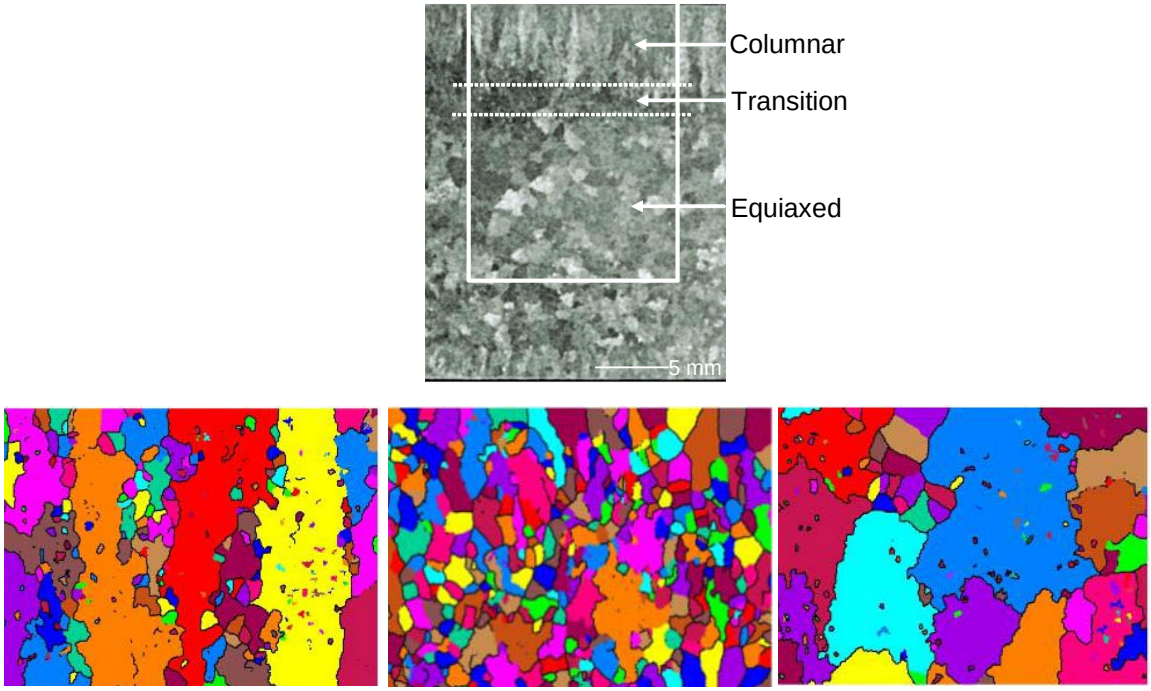

Figure 9: An optical macrograph showing different regions within an Al-Si casting in a step mould (top), and the corresponding grain colour maps obtained using electron back scatter diffraction for the columnar, transition and equiaxed regions respectively (bottom, from left to right).

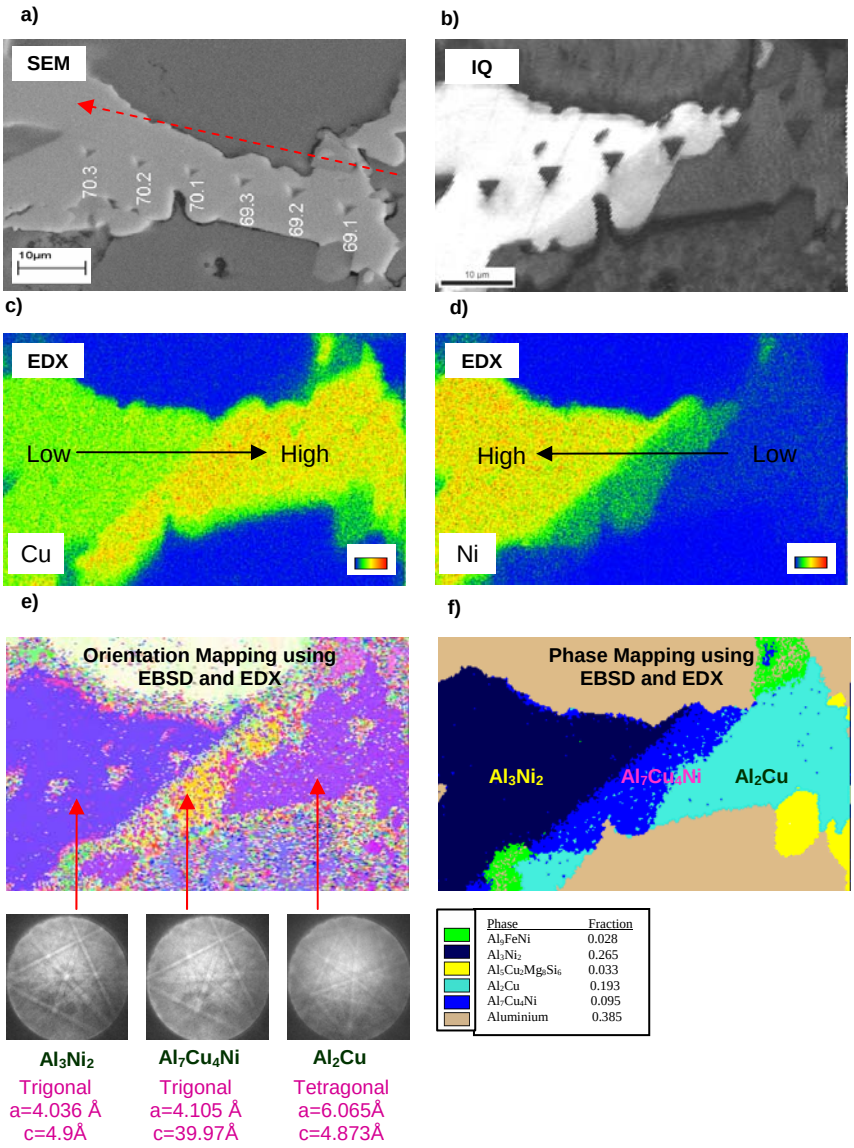

Figure 10: (a) An SEM image of an intermetallic particle in a multicomponent Al-Si alloy, (b) corresponding image quality map, EDX maps of (c) Cu and (d) Ni, orientation mapping (e) and phase mapping (f) using combined EDX and EBSD [36].

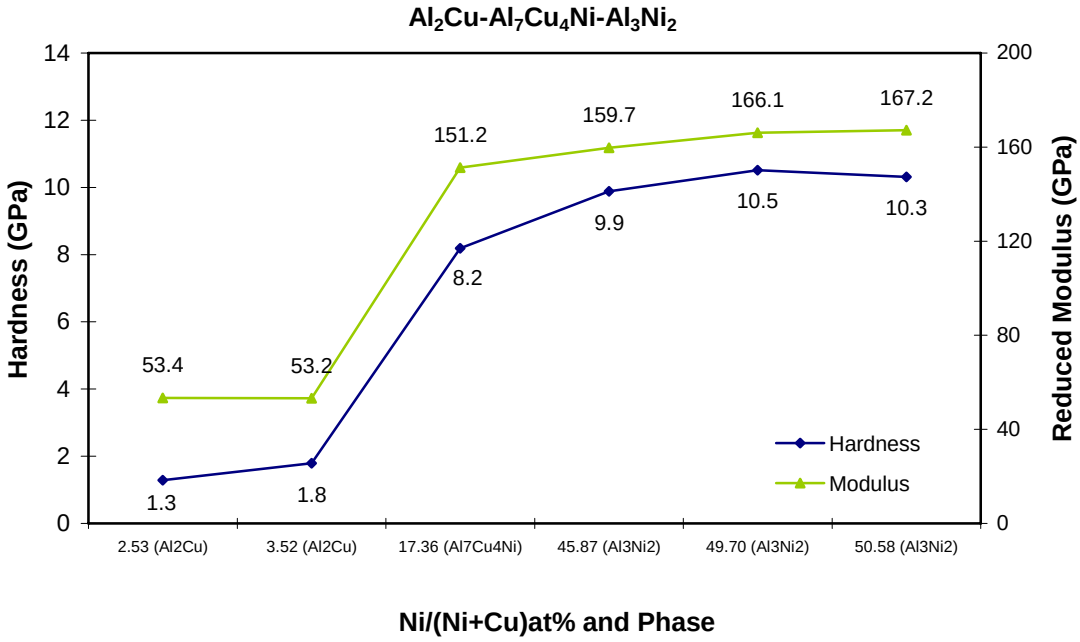

Figure 11: The hardness and reduced modulus of the particle shown in Figure 10 determined using nanoindentation [36].

Next Paper *Back to Programme*